

## Dependence on cation size of thermally induced capacitive effect of a nanoporous carbon

Hyuck Lim,<sup>1</sup> Weiyi Lu,<sup>2</sup> and Yu Qiao<sup>1,2,a)</sup>

<sup>1</sup>Program of Materials Science and Engineering, University of California – San Diego, La Jolla, California 92093, USA

<sup>2</sup>Department of Structural Engineering, University of California—San Diego, La Jolla, California 92093-0085, USA

(Received 22 May 2012; accepted 23 July 2012; published online 7 August 2012)

Nanoporous carbon based thermally chargeable supercapacitors (TCS) are characterized in a set of experiments for low-grade heat harvesting and storage. A TCS consists of two nanoporous electrodes immersed in an electrolyte solution. When the temperature of one of the electrodes rises, its electrode potential increases, and a significant amount of thermal energy is converted to electric energy. The temperature sensitivity of the electrode potential ( $|dV/dT|$ ) is highly dependent on the cation size: with everything else being the same, as the cation diameter ( $d$ ) decreases,  $|dV/dT|$  increases. © 2012 American Institute of Physics. [<http://dx.doi.org/10.1063/1.4742748>]

Harvesting and storing low-grade heat (LGH) is of both significant scientific interest and important technological relevance.<sup>1</sup> Usually, LGH refers to the thermal energy of heat sources below 250–300 °C. Everyday, in the United States alone, many hundreds of Giga-Watt of power is being wasted as LGH in coal and nuclear power plants.<sup>2</sup> Other LGH sources include solar thermal energy, geo-thermal energy, ocean thermal energy, wasted heat in vehicles, and even body temperature of human beings. If LGH can be utilized with a high energetic and economic efficiency, energy security can be much improved and energy-related emission can be greatly reduced.

Conventional thermal energy harvesting and storage techniques do not work well for LGH.<sup>2,3</sup> A major problem is the low energy density, making direct thermal energy storage methods, e.g., those based on phase transformations and/or chemical reactions,<sup>4</sup> irrelevant. An intrinsic difficulty of converting LGH to electricity comes from the low temperature, which leads to the low Carnot cycle limit,  $\zeta_c$ . Thus, the overall energy conversion efficiency  $\zeta = \zeta_c \cdot \zeta_s$  tends to be poor, with  $\zeta_s$  being the system efficiency. For large-scale LGH sources, neither direct energy conversion, e.g., thermoelectrics, nor indirect energy conversion, e.g., Organic Rankin Cycle (ORC) machines and turbine engines, can work efficiently.<sup>5</sup> To overcome these hurdles, new mechanisms must be investigated.

Converting thermal energy to electric energy must be based on processes that are both thermally and electrically related. Such processes usually involve multiple phases/matters and take place at their interfaces, and beneficial interface effects can often be amplified by using nanostructured materials of ultrahigh specific surface areas ( $A \sim 10^2$  to  $10^3$  m<sup>2</sup>/g). Among all the interfaces, solid-liquid interfaces should be given a high priority as they are quite controllable. A nanostructured-materials-based device that uses solid-liquid interfaces to store electric energy is essentially a double-layer supercapacitor (DLS). For instance, when two identical

nanoporous electrodes are soaked in an electrolyte solution and an external voltage is applied across them, the cathode would adsorb anions and the anode would adsorb cations. The stored charge can be assessed as  $Q = Q_e \cdot A$ , where  $Q_e$  is the effective surface ion density. Due to the large value of  $A$ ,  $Q$  can be much higher than that of many conventional capacitors.<sup>6</sup>

Note that the ion adsorption of DLS is also thermally dependent. It is well known that a “poorly designed” DLS can lose up to 20% of its capacitance with a small temperature variation.<sup>7</sup> While this is usually regarded as a detrimental effect, recently we showed that its inverse process can be employed to harvest and store LGH as electric energy, leading to the development of the thermally chargeable supercapacitor (TCS) technology.<sup>8</sup> The basic working mechanism of TCS is associated with the thermally induced variation of electrode potential. As depicted in Fig. 1(a), a possible structure of TCS consists of two identical half-DLS. Each half-DLS is formed by immersing a nanoporous electrode in an electrolyte solution. As they are placed at different temperatures ( $T$ ), there would be a potential difference ( $V$ ) between them, because the effective surface ion density changes with  $T$ . Since the temperature sensitivity of electrode potential,  $|dV/dT|$ , is much higher than the Seebeck coefficients of thermoelectric materials, a TCS can have a high energy density. Moreover, as the two half-DLS are separated, direct thermal conduction between them can be minimized, so that thermal shorting, the key factor that causes the low energetic efficiency of the Seebeck effect,<sup>9</sup> is significantly reduced.

While the preliminary data have shown encouraging results, in order to optimize TCS, a large number of technical and scientific questions must be answered. A critical issue is: How to choose the electrolyte? A recent experiment showed that the output voltage of TCS is highly dependent on the anion size.<sup>10</sup> At a large electrode surface, if anions are the dominant species, the cation effects should be secondary. However, our experimental data indicate that the cation effects are even more pronounced, as will be discussed below.

<sup>a)</sup>Author to whom correspondence should be addressed. E-mail: yqiao@ucsd.edu.

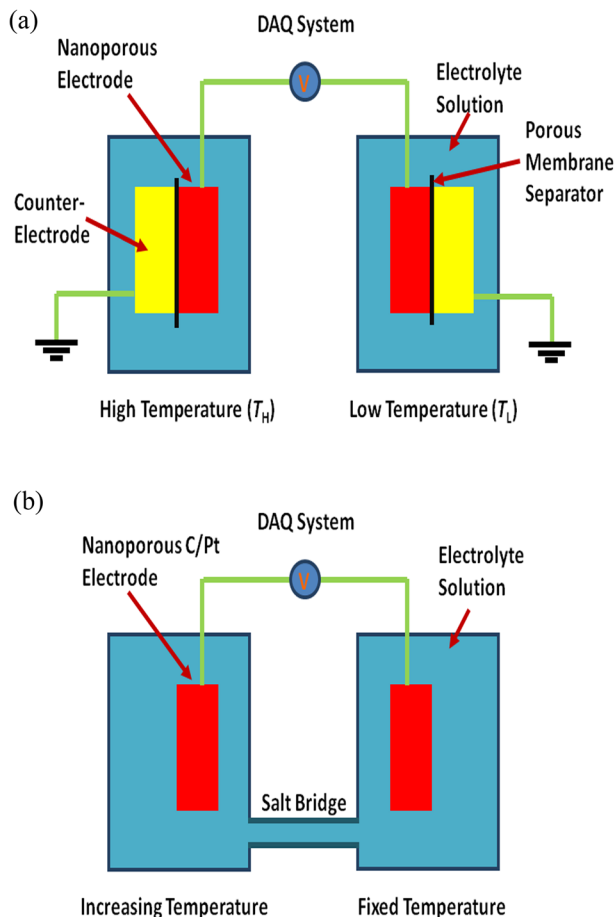


FIG. 1. Schematics of (a) the thermally chargeable supercapacitor (TCS) and (b) the experimental setup.

The electrode under investigation was formed by Cabot BP2000 nanoporous carbon (NC). The material was refluxed in a vertical reactor in acetone for 4 h. The refluxing temperature was kept at 60 °C by a hot mantle. After vacuum drying at 80 °C for 8 h, the treated NC powders were compressed into thin disks by a type-5580 Instron machine in a stainless steel mold. The mass of each disk was nearly 200 mg. The compression pressure was 400 MPa. By using a Micrometrics ASAP-2000 Analyzer, it was measured that the compressed carbon had a broad pore size ( $D$ ) distribution from 1 nm to 100 nm, with the modal value at about 3 nm. The smallest nanopores with  $D < 10$  nm contributed to more than 85% of the surface area.

The schematic of the experimental setup is shown Fig. 1(b), which is similar with the one in Fig. 1(a) except that the counter-electrode and the grounding connections were replaced by a salt bridge. The diameter of the salt bridge was 5 mm, and the length was 30 mm. The two containers were made of polypropylene (PP). Each container contained 50 ml of aqueous solution of electrolyte. The electrolyte concentration was either 0.1 M or 3.7 M. The electrolyte was either lithium chloride (LiCl), sodium chloride (NaCl), potassium chloride (KCl), or cesium chloride (CsCl).

The two NC disks were connected to a National Instrument SCB68 data acquisition (DAQ) system by platinum (Pt) wires through two Pt charge collectors. One container was maintained at room temperature by a water bath. The

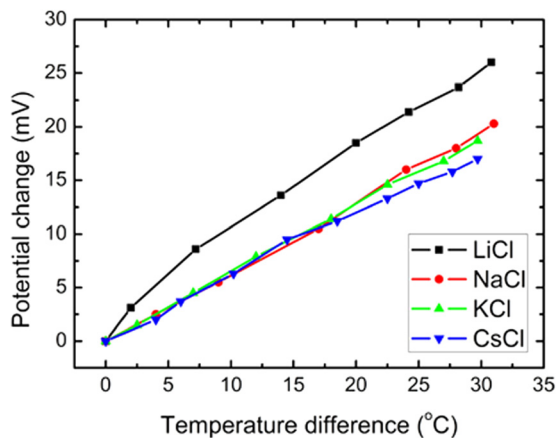


FIG. 2. Typical results of the output voltage ( $V$ ) as a function of the temperature difference ( $\Delta T$ ). The ion concentration is kept as 0.1 M.

other container was heated by a Corning PC-220 Hot Plate, with the heating rate of 3 °C/min. The DAQ system continuously recorded the potential difference between the high-temperature and the room-temperature NC disks. Fig. 2 shows the typical measurement results. The average  $dV/dT$  is shown in Fig. 3 as a function of the diameter of cation ( $d$ ) and the ion concentration ( $C$ ). According to the literature data,<sup>11</sup> the ion diameters of  $\text{Li}^+$ ,  $\text{Na}^+$ ,  $\text{K}^+$ , and  $\text{Cs}^+$  are 0.180 nm, 0.232 nm, 0.304 nm, and 0.362 nm, respectively. In the control experiment, the NC disks were removed, and only the Pt plates were tested as electrodes, with everything else remaining the same.

Figure 2 indicates clearly that the effective electrode potential is highly sensitive to temperature,  $T$ , for all the tested chloride salts. Initially, when both containers are at

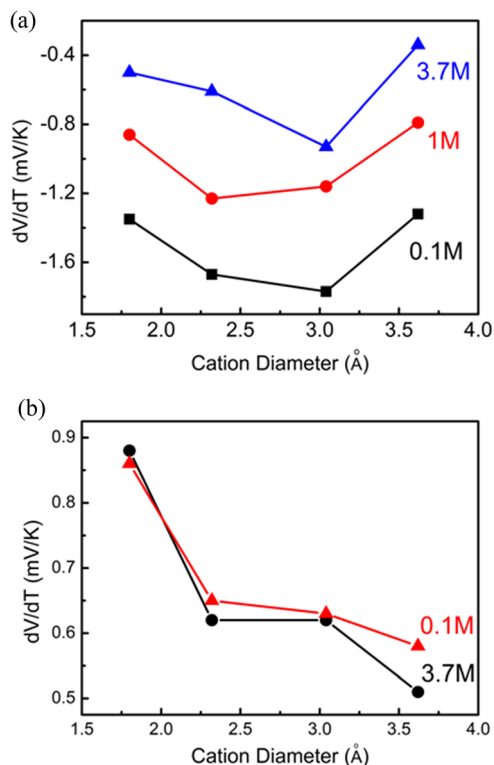


FIG. 3. The average value of  $|dV/dT|$  as a function of the cation size,  $d$ , of the Pt electrode and (b) the nanoporous carbon electrode.

room temperature, the potential difference is zero, as it should be. When the temperature difference ( $\Delta T$ ) increases, the electrode potential of the room-temperature NC disk remains constant, while that of the high-temperature NC disk rises, causing the measured output voltage ( $V$ ). The values of  $|dV/dT|$  are on the scale of 0.5–0.9 mV/°C, higher than that of solid-state thermoelectrics by at least an order of magnitude. The  $V$ - $T$  relationship is quite linear, suggesting that the mechanism of electrode potential variation is the same across the temperature range under investigation.

Note that Pt and NC electrodes exhibit different characteristics of thermal dependence of electrode potential, as shown in Figs. 3(a) and 3(b). First, the electrode potential of NC increases with temperature, while that of Pt decreases. Usually, at a higher temperature, the effective surface ion density is lower, as more ions can diffuse away from the Helmholtz plane.<sup>12</sup> The different trends in NC and Pt behaviors suggest that ions of opposite charges dominant their electrode potentials, which may be related to the surface moieties on the NC surface. During the preparation of the highly porous NC, significant oxidation takes place,<sup>13</sup> as carboxylic and/or hydroxyl groups are formed. These surface groups are negatively ionized in solution, attracting cations and repelling anions. On the contrary, near the Pt surface, anions can be adsorbed.<sup>14</sup> The preference of the carbon nanopore for cations makes the cation size effect more pronounced compared to the previously reported anion size effect.<sup>10</sup> The sensitivity of  $|dV/dT|$  to the ion size are 0.15 ~ 0.19 mV/Å·K and ~0.09 mV/Å·K for cations and anions, respectively. Second, from Figs. 3(a) and 3(b), it can be seen that  $dV/dT$  of the NC is dependent on the cation diameter, while that of Pt is not. This phenomenon can be associated with the previous discussion that anion is the dominant specie for the Pt electrode, and in all the tests, the anion species and concentration are the same. For the NC electrode, different cations dominate  $dV/dT$ .

In the current study, most of the important system parameters are maintained the same, including the cation and anion charge, the ion concentration, the anion specie, the solvent, the electrode material, and the testing condition. The only major difference is the cation size, varying from  $\text{Li}^+$  to  $\text{Cs}^+$ . The experimental data show that  $|dV/dT|$  decreases monotonically as the cation diameter ( $d$ ) increases. In both dilute (0.1 M) and high-concentration (3.7 M) solutions,  $|dV/dT|$  is nearly 0.85 mV/°C for lithium salt and decreases to about 0.52 mV/°C for the largest cesium salt, by almost 40%. The relationship between  $|dV/dT|$  and  $d$  is nonlinear. When the cation changes from lithium to sodium and from potassium to cesium, the decrease in  $|dV/dT|$  is quite evident. The difference between sodium and potassium cations is within the tolerance of measurement.

The electrode potential can be described as:<sup>15</sup>  $\phi = (\phi_e - \phi_{\text{IHP}}) + (\phi_{\text{IHP}} - \phi_b)$ , where  $\phi_e$ ,  $\phi_{\text{IHP}}$ , and  $\phi_b$  are the potentials of the electrode surface, the IHP, and the bulk liquid phase, respectively. The potential drops can be expressed in terms of integral capacities ( $K$ ); thus,  $\phi = Q_e/K_e + Q_{\text{IHP}}/K_{\text{IHP}}$ , where  $Q$  is the surface charge and the subscripts “e” and “IHP” indicate the electrode-IHP system and the IHP-bulk system, respectively. The overall interface capacitance is  $C_i = dQ_e/d\phi$ . Note that  $Q_e = Q_{\text{CA}} + Q_{\text{IHP}}$ , with

$Q_{\text{CA}}$  being the charge associated with the specifically adsorbed ions, and, consequently,  $1 = dQ_{\text{CA}}/dQ_e + dQ_{\text{IHP}}/dQ_e$ . Therefore,  $1/C_i = 1/K_e - (1/K_{\text{IHP}})(dQ_{\text{CA}}/dQ_e)$ . Since the IHP structure may be simplified as a monolayer,  $Q_{\text{CA}}$  is linear to the adsorption coverage ( $\theta$ ):  $Q_{\text{CA}} = \alpha \cdot \theta$ , with  $\alpha$  being a system constant. Hence,  $\phi = (1/K_e + 1/K_{\text{IHP}}) \alpha d\theta$ . As a first-order approximation, the adsorption behaviors can be described by a Temkin isotherm:<sup>16</sup>  $\theta = \ln \beta c f = (k_B T/B) \ln [c \cdot \exp(Q_o/k_B T)]$ , where  $k_B$  is Boltzmann constant,  $B$  is a system constant related to the heat of adsorption, and  $Q_o$  is the heat of adsorption. Thus,  $d\theta/dT = (k_B \ln c)/B + (dQ_o/dT)/B$ . We can then derive the equation for the temperature sensitivity

$$\left| \frac{dV}{dT} \right| = - \frac{1}{K_{\text{IHP}} B} \left( k_B A \ln c + \frac{dQ_o}{dT} \right). \quad (1)$$

In Eq. (1), the first term in the bracket on the right-hand side (RHS) is not related to the cation size. The second term reflects the change in heat capacity of the adsorbate before and after the adsorption, which can be regarded as the change in heat capacity ( $\Delta C$ ).<sup>17</sup> Usually, a smaller ion tends to have a higher degree of hydration, causing a more pronounced change in heat capacity.<sup>18</sup> That is, smaller cations with more hydration molecules would have a higher degree of freedom than bigger ones.<sup>19</sup> Thus, the larger the value of  $dQ_o/dT$ , the higher the temperature sensitivity ( $dV/dT$ ) would be.

The phenomenon that both cations and anions have significantly influence on the TCS performance may also be associated with the confinement effect of the nanopore walls: As the interior of a nanopore is relatively small compared with the interface zone, both cations and anions are confined in the nanoenvironment, somewhat in direct contact with the inner surfaces.

Another interesting phenomenon is that, when the ion concentration increases from 0.1 M to 3.7 M by more than an order of magnitude, the temperature sensitivity of electrode potential and its dependence on cation size do not vary much, suggesting that the ion concentration in NC is not the critical factor affecting  $dV/dT$ .

Clearly, detailed analysis on thermally induced ion adsorption and desorption in nanopores must be carried out to fully understand the TCS performance. Nevertheless, the current testing data suggest that using different cations can significantly affect the TCS behaviors. When the cation size increases, with everything else being the same,  $|dV/dT|$  decreases. The influence of the cation concentration is secondary.

This work was supported by the National Science Foundation under Grant No. ECCS-1028010.

<sup>1</sup>A. Kapil, I. Bulatov, J. Kim, and R. Smith, *Chem. Eng. Trans.* **21**, 367 (2010).

<sup>2</sup>R. H. Lasseter and P. Paigi, “Microgrid: A conceptual solution,” in *35th Annual IEEE Power Electronics Specialists Conference* (2004), pp. 2521–2525.

<sup>3</sup>R. J. Krane, *Energy Storage Systems* (Kluwer Academic, Dordrecht, 1989), pp. 37–67.

<sup>4</sup>B. Zalba, J. M. Marin, L. F. Cabeza, and H. Mehling, *Appl. Therm. Eng.* **23**, 251–283 (2003).

<sup>5</sup>E. Barbier, *Renew. Sustain. Energy Rev.* **6**, 3–65 (2002).

- <sup>6</sup>A. Peigney, Ch. Laurent, E. Flahaut, R. R. Bacsa, and A. Rousset, *Carbon* **39**, 507 (2001).
- <sup>7</sup>C. E. D. Chidsey, *Science* **251**(4996), 919–922 (1991).
- <sup>8</sup>Y. Qiao, V. K. Punyamurtal, A. Han, and H. Lim, *J. Power Sources* **183**, 403–405 (2008).
- <sup>9</sup>I. Sur and A. Casian, *Phys. Rev. B* **69**, 035306 (2004).
- <sup>10</sup>H. Lim, W. Lu, A. Han, and Y. Qiao, *Int. J. Electro Chem. Sci.* **7**, 2577–2583 (2012).
- <sup>11</sup>S. S. Zumdahl and S. A. Zumdahl, *Chemistry*, 8th ed. (Charles Hartford, 2010), Chap. 8.
- <sup>12</sup>A. J. Bard and L. R. Faulkner, *Electrochemical Methods—Fundamentals and Applications* (John Wiley & Sons, INC.), Chap. 12, pp. 566–567.
- <sup>13</sup>J. Barkauskas and M. Dervinyte, *J. Serb. Chem. Soc.* **69**(5), 363–375 (2004).
- <sup>14</sup>A. M. Abd El-Halim, M. I. Sobahi, and A. O. Baghlaf, *Surf. Technol.* **18**, 225 (1983).
- <sup>15</sup>J. O'M Bockris, A. K. N.Reddy, and M. Gamboa-Aldeco, *Modern electro-chemistry 2A-Fundamentals of Electroics* (Springer), Chap. 6, p. 872.
- <sup>16</sup>A. Frumkin and A. Slygin, *Acta Physicochimica U.R.S.S.* **3**, 791 (1935).
- <sup>17</sup>Y. Huang, *J. Catal.* **25**, 131–138 (1972).
- <sup>18</sup>J. O'M Bockris, A. K. N.Reddy, and M. Gamboa-Aldeco, *Modern Electro-chemistry, Vol. 1, Ionics* (Springer), Chap. 2, p. 71.
- <sup>19</sup>D. Shen and M. Bulow, *Adsorption* **6**, 275–286 (2000).